Design of a Noninvasive Magnetic Hyperthermia System for Breast Tumors Using Fe3O4 Nanoparticles

Maged A.Yahya*, Sulafa Y. Ahmed*, Faihaa M. Eltigani, Mawahib G. Abdalrahman,

Electronics Engineering Department, University of Gezira, Sudan
E-mail: sulafa174@gmail.com

* Equal contributors: Sulafa. Y. M. Ahmed and Magid. A. A. Yaya

Received:26/09/2021
Accepted:21/12/2021

ABSTRACT- Breast cancer is the second leading cause of death among women in the 40 – 55 age group. There are many methods to treat breast cancer, such as chemotherapy and radiation, but they have many side effects, such as hair loss and weakness. Magnetic hyperthermia is a modality that gives new hope for cancer treatment with minimum side effects. This technique relies on raising the temperature of the tumor to 41- 45°C by the alternating magnetic field generated from the magnetic coil. This study aims to design a suitable magnetic hyperthermia system comprised of breast models with tumors and coil to be used as a source of alternating magnetic field. First, the magnetic coil was designed and tested, and then six 3D breast models were created. These models differ in the number of layers and the position of the tumor. Fe3O4 magnetic nanoparticles (MNPs) were added to each tumor. After that, the magnetic coil was tested on the models and temperature elevation and distribution were calculated. The tumor near the surface reached a temperature of 44.2 ºC and the deep tumor had a temperature of 42.5 ºC while the surrounding tissues remain at safe temperature ranges. The results showed the capability of the designed coil to raise the temperature of breast tumors to the therapeutic range.

Keywords*: Breast cancer, Magnetic hyperthermia, Pennes' equation, Fe3O4 nanoparticles.*

المستخلص – سرطان الثدي هو السبب الرئيسى الثاني لوفيات النساء في الفئة العمرية من 40 الى 55 سنة. هناك العديد من الطرق لعلاج سرطان الثدي، مثل العلاج الكيميائي والإشعاعي، ولكن لهذه الطرق العديد من الآثار الجانبية، مثل تساقط الشعر والضعف العام. العلاج الحراري المغنطيسي هو احد انواع علاج السرطان بأقل آثار جانبية. تعتمد هذه التقنية على رفع درجة حرارة الورم إلى 41–45 درجة مئوية بواسطة المجال المغناطيسي المتردد و المتولد من ملف مغناطيسي. تهدف هذه الدراسة إلى تصميم نظام حراري مغناطيسي يتألف من نماذج ثدي بها أورام وملف لاستخدامه كمصدر للحقل المغناطيسي المتردد. أولاً ، تم تصميم الملف المغناطيسي واختباره ، ثم تم تصميم ستة نماذج ثدي ثلاثية الأبعاد. تختلف هذه النماذج في عدد الطبقات وموقع الورم. تمت إضافة جزيئات الحديد النانوية المغناطيسية من نوع Fe3O4 إلى كل ورم. بعد ذلك، تم اختبار الملف المغناطيسي على كل النماذج وتم حساب ارتفاع درجة الحرارة وتوزيعها. وصلت درجة حرارة الورم القريب من السطح إلى 44.2 درجة مئوية ، بينما كانت درجة حرارة الورم العميق الى 42.5 درجة مئوية بينما بقيت الأنسجة المحيطة في درجات حرارة آمنة. أظهرت النتائج قدرة الملف المصمم على رفع درجة حرارة أورام الثدي إلى النطاق العلاجي.

Introduction

According to the World Health Organization, breast cancer was classified as the world's most prevalent cancer in 2020. There were 2.3 million women diagnosed with breast cancer and 685 000 deaths globally. As of the end of 2020, about 7.8 million women diagnosed with breast cancer in the past five years [1].

There are many treatment methods for breast cancer such as chemotherapy and radiotherapy, but they have many side effects such as pain, hair loss, weight gain/loss, early menopause, loss of appetite, nausea, weakness, mouth sores, diarrhea, high risk of infection and inflict deep anxiety [2]. For decades, researchers have been exploring new safe technologies for breast cancer treatment [2]. Hyperthermia is a technology that has given new

hope for cancer treatment with minimum side effects on the patient. Many clinical researches have shown the beneficial effect of hyperthermia [2]. As a new method for cancer treatment, hyperthermia has already entered clinical practice [3].

Hyperthermia therapy is a treatment modality used with other treatments (such as chemotherapy) to treat cancer, where the tumors are exposed to high temperatures. This heating is generated from devices from inside or outside the body - depending on the location of the tumor [4]. Hyperthermia can be defined more precisely as killing the cancer cells by raising the temperature of a part of the body or whole body to (41– 45°C) for a specified time [5]. These high temperatures lead to damage and killing of cancer cells with a reversible effect on the surrounding healthy cells.

There are many types of hyperthermia like microwave hyperthermia, radiofrequency hyperthermia, ultrasound hyperthermia, and Magnetic hyperthermia (MHT). These techniques have many limitations, like shallow penetration [6]. The main advantages of magnetic hyperthermia over other types: uniform heating and deep penetration.

During magnetic hyperthermia treatment, a drug that contains magnetic nanoparticles (MNPs) is injected into the body of the patient, then an external alternating magnetic field (AMF) is applied (through a device such as a coil) near the tumor position. AMF is absorbed by the MNPs in the tissue and generates an electric eddy current that generates heat and raises the tumor temperature [7]. The amount of generated heat depends on many factors such as frequency and strength of the magnetic field, nanoparticle size and composition, and concentration within the tissue [8].

Magnetic nanoparticles (1-100 nanometers in diameter) are a class of nanoparticles that can be controlled using external magnetic fields [9]. To obtain the required heating, the alternating magnetic field typically should have a frequency in the range between 100 kHz and 500 kHz [10].

Many studies designed magnetic hyperthermia systems using simple models with simple models of tumors and breasts [11-15]. Using a simple model could not reflect the actual process when using a realistic model. This study aims to design a magnetic hyperthermia system using 3D multiple-layer breast models containing a tumor.

Material and Methods

The breast tumor was injected with uniformly distributed MNPs and, the coil was designed to generate magnetic waves. The generated waves were used to stimulate the MNPs inside the tumor, and then elevate its temperature. We performed the following steps: the coil was designed and used to generate the alternating magnetic field; six breast models were created; a small tumor was added to each model - in different locations; the material properties for breast, tumor, and MNP were assigned; the designed coil was tested in the breast models.

All the simulations were performed using Computer Simulation Technology (CST) software [16]. Two solvers of the CST were used. The Electromagnetic Solver was used to calculate the amount of absorbed energy by breast and tumors due to the AMF; and the Thermal Solver which used to calculate the temperature distribution in the models.

Coil design

A coil is a passive component that stores energy in a magnetic field surrounding it when electric current flows through it. In MHT, the coil is the primary source that affects the MNPs to produce heat. In this work, a copper coil was designed (Fig.1) with design parameters shown in Table 1.

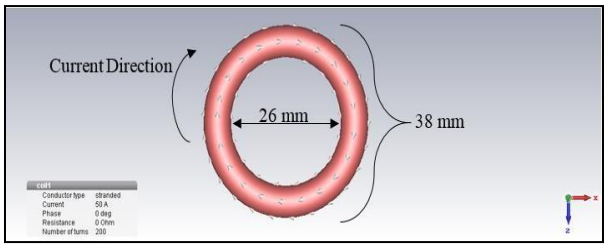

Figure 1. Coil configuration

TABLE 1: PARAMETERS OF THE COIL

Parameters	Value
Current	50 Ampere
Turns Number	200
Frequency	100 KHz
Internal diameter	26 mm
Outer Diameter	38 mm

Breast models

The breast model was created in CST software. The model has a hemispherical shape with a radius equal to 50 mm. Based on this model six models were generated. These models differ according to the number of layers and the tumor location as

illustrated in Fig 2 to Fig.7. In this study, a spherical tumor with a radius of 2.5 mm was used. Inside the tumor, MNPs were added with a size of 100 nm. These nanoparticles have been distributed throughout the tumor.

Figure 2 shows a simple breast model (model A). This model consists of a single layer of fat and has a tumor close to the surface. Figure 3 shows the breast model after adding the skin layer with a thickness of 1.5 mm (model B). To model a similar structure to a realistic breast, a glandular tissue was added as shown in Figure 4 (model C). Figure 5 shows (model D) where the tumor in model C was placed close to the edge. Figure 6 shows model E, where the tumor was placed in a deeper site within the glandular tissue and away from the breast surface. The effect of nanoparticles was studied by using a model (F) without MNPs (Figure 7).

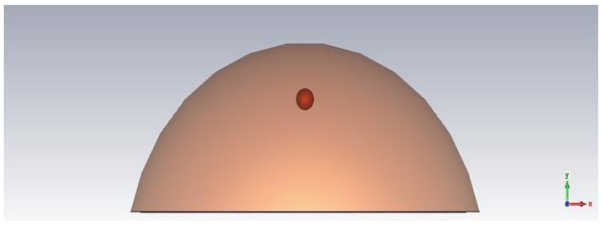

Figure 2. Model A (single layer of fat with a tumor close to surface)

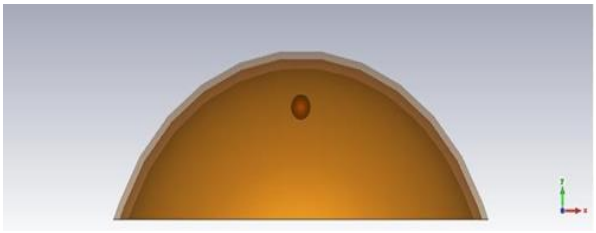

Figure 3. Model B (fat and skin layers)

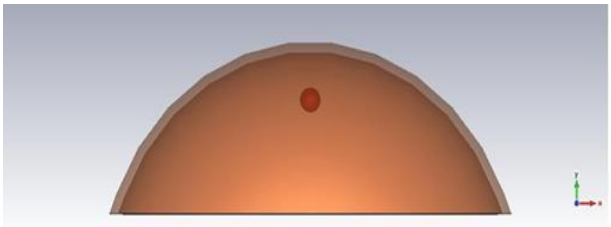

Figure 4. Model C (fat, skin, and gland layers)

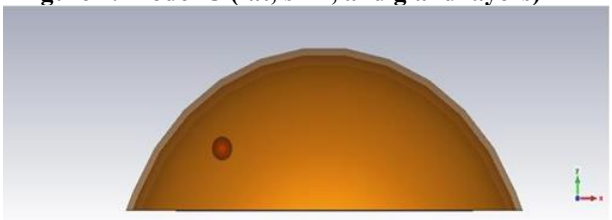

Figure 5. Model D (fat, skin, and gland layers with edge tumor)

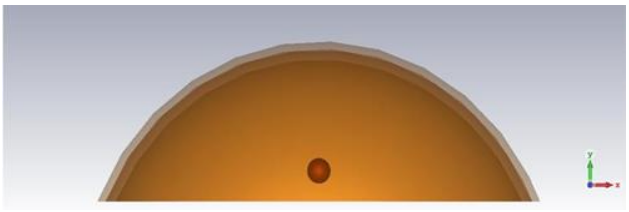

Figure 6. Model E (fat, skin and gland layers with deep tumor

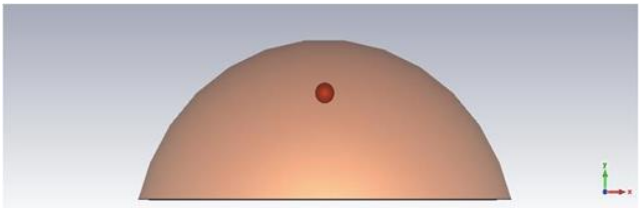

Figure 7. Model F (fat layer without MNPs in the tumor)

Assigning material properties

After the modeling process, the properties of the material were assigned to the model's layers. These properties are classified into dielectric properties - conductivity and relative permittivity - and thermal properties -thermal conductivity, heat capacity, and density.

There is a material library in CST which includes bio tissue materials like breast fat, breast gland, liver, blood, and bone. Some properties were taken from the CST library and others from the literature [17-29]. Since the dielectric properties of different tissues changed with frequency [30], all properties were selected at 100 kHz (operating frequency of the used magnetic field). Tables 2 and 3 show the dielectric and thermal properties of the breast model, respectively.

TABLE 2: DIELECTRIC PROPERTIES OF BREAST MODEL (AT 100 KHZ)

Materials	Electrical conductivity (σ) (s/m)	Relative permittivity (ε_r)
Skin	0.065836	15357
Fat	0.082490	276
Gland	0.537000	3300
Tumor	0.644160	3358

One of the basic concepts in hyperthermia is that cancer cells are more sensitive to heat than healthy cells [31]. Blood flow coefficient (BFC) and basal metabolic rate (BMR) are predominant features that distinguish malignant and healthy cells.

TABLE 3: THERMAL PROPERTIES OF BREAST MODEL (AT 100 KHZ)

Materials	Thermal conductivity (k) $(W/m/K)$	Heat capacity (cp) $(kJ/kg/K)$	Density (ρ) (kg/m^3)
Skin	0.37	3.391	1109
Fat	0.21	2.348	911
Gland	0.49	2.960	1058
Tumor	0.55	3.1	1060

The BFC represents the scattered energy generated by the flowing of blood through tissues; the BMR represents the generating energy produced by metabolic activities [32]. To study the effect of both factors, the properties of tumor and breast tissues were included as illustrated in Table 4.

Studies show that blood flow coefficients in the tumor are low compared to normal cells (only 5% compared to normal tissue) [33]. When the tumor exposes to electromagnetic energy, the heat produced will make the BFC stagnant in the local area [34].

When the tumor temperature reaches 41°C to 45 °C, the blood flow stops in the tumor, and the mitochondria in tumor cells appear vacuolation which kills the tumor cells [35]. The metabolic rate for cancer cells is higher than normal cells; according to previous studies, the value of metabolic activity in breast tumors varies between 13,000 and 70,000 [26], [27] and [28].

TABLE 4: BLOOD FLOW COEFFICIENT (BFC) AND BASAL METABOLIC RATE (BMR) OF BREAST MODEL

Materials	BFC $(W/m^3/K)$	BMR (W/m^3)
Skin	800	400
Fat	1700	400
Gland	2400	700
Tumor	85	13000 – 70000

After assigning the material properties for both breast tissues and tumor, the Fe3O4 nanoparticles were added to the tumor. Fe3O4 nanoparticles were selected since they are widely used in diagnostic and therapeutic applications because of their low cost, tunable properties, and biocompatibility [36].

Table 5 shows the dielectric and thermal properties of MNPs (Fe3O4) [37, 38]. In all models, none of the coil parameters have been changed. The coil was mover closer to the tumor - in the model containing a tumor at the edge.

TABLE 5: DIELECTRIC AND THERMAL PROPERTIES OF FE3O4 MNPS

Properties	Value
Relative permittivity (ε_r)	100
Electrical conductivity (σ)	25000 S/m
Thermal conductivity (k)	6 W/m/K
Heat capacity (c_b)	0.67 kJ/kg/K
Density (ρ)	5200 kg/m^3

Testing the coil on the breast models (complete system)

The proposed system (Fig 8) consists of a coil to produce an AMF and breast model with a three-layer, the skin layer with a thickness of 1.5 mm, the fat layer with a thickness of 2 mm, the gland layer, and a tumor with 2.5 mm radius

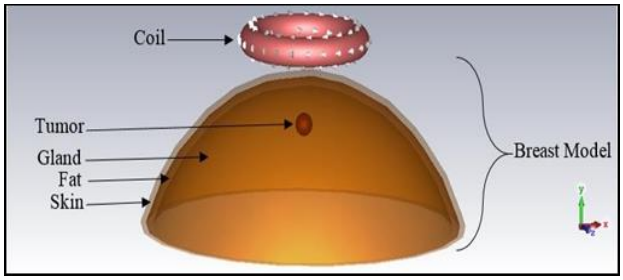

Figure 8. Hyperthermia system Configuration

The simulations for the complete system were run in CST, where a low frequency (LF) domain solver was used to calculate the coil parameters such as a magnetic and electric field.

Then, the thermal solver (steady-state solver) was used to convert the absorbed power into temperature values taking into account effects of living tissue such as metabolic heating and blood flow influence.

Results

In this study, a magnetic hyperthermia system was designed, where; a coil generates an alternating magnetic field that affects nanoparticles inside the breast tumor. This effect increases the temperature of the medium containing these particles. Different temperatures values and distributions in all models were calculated. Figure 9 shows the temperature distribution in a one-layer model (model A).

Figure 10 shows the heat distributions in model B. Figure 10 represents the heat distribution in model C. Figure 12 shows the temperature distribution in model D. Figure 13 shows the temperature model E when the tumor is deeper. Figure 14 shows the temperature in model F (without MNPs).

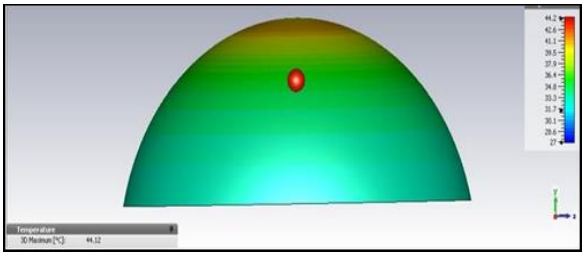

Figure 9. Temperature distribution in model A

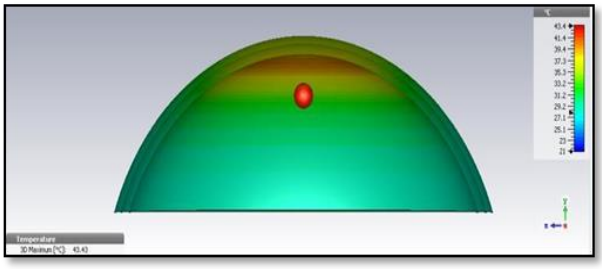

Figure 10. Temperature distribution in model B

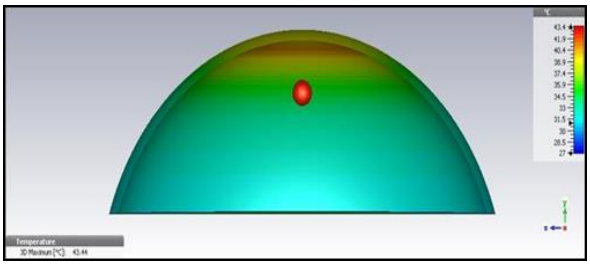

Figure 11. Temperature distribution in model C

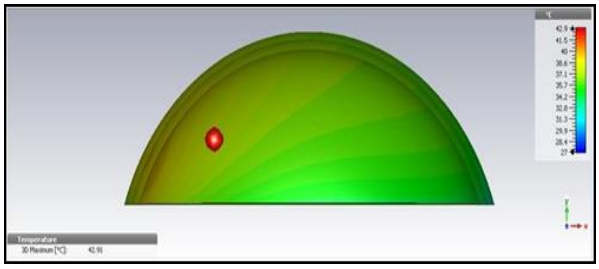

Figure 12. Temperature distribution in model D

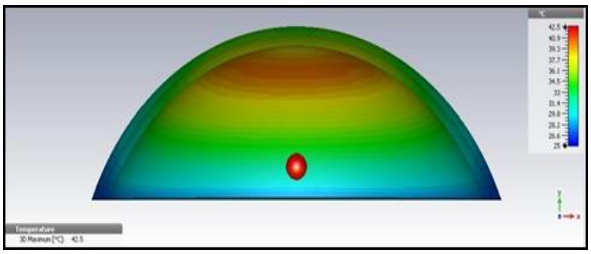

Figure 13. Temperature distribution in model E

Discussion

This study aimed to design a magnetic hyperthermia system capable of heating breast tumors to the therapeutic range of hyperthermia (41- 45°C). The proposed design showed the capability of raising the tumor temperature to more than 42 ºC, which is sufficient to destroy the tumor.

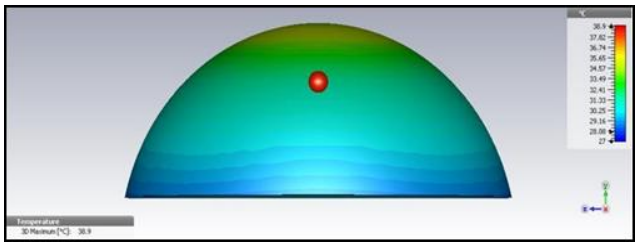

Figure 14. Temperature distribution in the model withoutMNPs

The coil's parameters and tumor size remained constant in all models. Six breast models were designed a one-layer model (model A); a two-layer model (model B); a three-layer model (model C); a three-layer model with a tumor in the edge (model D); a model with a deep tumor (model E); and a model without MNPs (model F).

Values and distribution of the tumor's temperature were affected by several factors: the number of breast layers, the location of the tumor, the presence of MNPs, and the magnetic field strength. All these factors will be discussed in the following paragraphs.

The effect of the model's structure

Several models were used to observe the effect of changing the structure (number of layers and location of the tumor). In model A (Fig 9), which contains fat only, it could be observed that the temperature is uniformly distributed and the maximum value is in the tumor, and there is increasing in temperature near the surface where the coil is placed.

These results have coincided with many other studies that used simple breast models [11-15]. Also, it could be observed that the tumor temperature in model A is higher than that of model B (Fig 10), which contains a skin layer since the skin acts like a heat dissipater. In model C (Fig 11), the tumor temperature did not change, but the gland layer has a high temperature compared to the skin and fat layers because of its high conductivity.

The effect of changing tumor location

In many previous studies [12, 13] and [21], the site of the tumor was not changed, but superficial tumors were used. In this study, different locations were tested. In model D and model E, the tumor location was changed. In model D, the tumor was placed at the edge and the coil position was changed to be suitable

for the tumor's new location. In model E, the tumor was placed in depth.

It could be observed even that temperature of the tumor in model D (Fig 12) reached the hyperthermia therapeutic range, but it is below other models because the direction of the magnetic field is not vertical and does not directly affect the tumor. In model E (Fig 13), we could observe that even the tumor is in a deep location; its temperature reached the therapeutic level. On the other hand, due to the relatively long distance of the tumor from the coil, the temperature of the majority of the breast tissues has increased.

The effect of MNPs

As previously explained, the resulting heat in the tumor is due to the interaction between the nanoparticles and the alternating magnetic field generated from the coil. Fig 14 illustrates the result of temperature in a nanoparticle-free model. Note that the temperature of the tumor is less than 40 ℃, but higher than normal tissues temperature due to the high metabolic rate of the tumor (0.5 to 2 ℃ higher than the surrounding tissues) [39].

The effect of AMF strength

Increasing of the strength of the alternating magnetic (controlled by current and number of turns) field increases the temperature of both breast and tumor and vice versa. So, it is important to tradeoff between used current and desired temperature. In this study, using of 50 Amp and 200 turns made this tradeoff which is suitable to the used tumor size.

Conclusions

This study presents a design of a low-cost, simple design magnetic hyperthermia system for the non-invasive treatment of breast tumors. The results proved the capability of the proposed setting to heat the tumors (closer to the surface or deeper) to the therapeutic ranges. Future work may include testing different tumor sizes and more complicated breast models.

References

[1] WHO. (5 August 2021). *World Health Organization. Breast Cancer*. Available: https://www.who.int/news-room/ fact-sheets/detail/breast-cancer.

[2] M. Sethi and S. Chakarvarti, (2015) "Hyperthermia Techniques for cancer treatment: A Review", *International Journal of PharmTech Research,* vol. 8, pp. 292-299.

[3] D.Sardari and N. Verga, (2011) "Cancer treatment with hyperthermia,"*Current Cancer Treatment-Novel Beyond Conventional Approaches*, ed: IntechOpen.

[4] K. Hynynen and B. Lulu, (1990) "Hyperthermia in cancer treatment", *Investigative radiology,* vol. 25, pp. 824-834.

[5] R. W. Habash, R. Bansal, D. Krewski, and H. T. Alhafid, (2006) "Thermal therapy, part 2: hyperthermia techniques," *Critical Reviews™ in Biomedical Engineering,* vol. 34.

[6] Tang Yuan, 2010. Cancer therapy combining the modalities of hyperthermia and chemotherapy: In vitro cellular response after rapid heat accumulation in the cancer cell (Doctoral dissertation, Florida International University).

[7] M. Kohani, M. Talebi, and M. B. Shafii, (2011) "Modeling and optimizing the temperature distribution around cancerous tissues during magnetic hyperthermia treatment", in *Proceedings of the international conference on modeling, simulation and visualization methods (MSV)*, p. 1.

[8] C. Zhang, D. T. Johnson, and C. S. Brazel, (2008) "Numerical study on the multi-region bio-heat equation to model magnetic fluid hyperthermia (MFH) using low Curie temperature nanoparticles", *IEEE transactions on nanobioscience,* vol. 7, pp. 267-275.

[9] M. Tadic, S. Kralj, M. Jagodic, D. Hanzel, and D. Makovec, (2014) "Magnetic properties of novel superparamagnetic iron oxide nanoclusters and their peculiarity under annealing treatment", *Applied Surface Science,* vol. 322, pp. 255-264.

[10] C. S. Kumar and F. Mohammad, (2011) "Magnetic nanomaterials for hyperthermia-based therapy and controlled drug delivery", *Advanced drug delivery reviews,* vol. 63, pp. 789-808.

[11] L. F. E. H. Silverio Soto Alvarez, Alma Verónica Vargas, Jaime López, and C. A. G. Jesus Gabriel Silva, (2016) "Characterization of Breast Cancer Radiofrequency Ablation Assisted with Magnetic Nanoparticles: In Silico and in Vitro Study", *Journal of Electromagnetic Analysis and Applications*.

[12] A. Miaskowski and A. Krawczyk, (2011) "Magnetic Fluid Hyperthermia for Cancer Therapy", *Electrical Review,* vol. 87, pp. 125-127.

[13] C. A. González, J. G. Silva, L. M. Lozano, and S. M. Polo, (2012) "Simulation of Multi-Frequency Induced Currents in Biophysical Models and Agar Phantoms of Breast Cancer", *Journal of Electromagnetic Analysis and Applications,* vol. 4, p. 317.

[14] S. M. Ali Rajabi, (2017) "Simulation of magnetic nanoparticle hyperthermia for curing the tumors using finite element method," presented at the Nanomedicine and Nanosafety Conference (NMNS 2017), Tehran University of Medical Sciences.

[15] T. Mustafa, Y. Zhang, F. Watanabe, A. Karmakar, M. P. Asar, R. Little, M. K. Hudson, Y. Xu, and A. S. Biris, (2013) "Iron oxide nanoparticle-based radio-frequency thermotherapy for human breast adenocarcinoma cancer cells", *Biomaterials Science,* vol. 1, pp. 870-880.

[16] CST, "CST STUDIO SUITE (2017).

[17] D. W. Ferreira and L. Lebensztajn, (2013) "A systematic sensitivity analysis of the performance of a transcutaneous energy transmitter for design purposes", *Journal of Microwaves, Optoelectronics and Electromagnetic Applications,* vol. 12, pp. 292-306.

[18] S. M. Hesabgar, A. Sadeghi-Naini, G. Czarnota, and A. Samani, (2017) "Dielectric properties of the normal and malignant breast tissues in xenograft mice at low frequencies (100 Hz–1 MHz)", *Measurement,* vol. 105, pp. 56-65.

[19] Gabriel. (23 january 1996). *Tissue Properties*. Available: https://itis.swiss/virtual-population/tissue-prope rtie s/ da ta base/dielectric-properties/.

[20] H. Wang, J. Wu, Z. Zhuo, and J. Tang, (2016) "A three-dimensional model and numerical simulation regarding thermoseed mediated magnetic induction therapy conformal hyperthermia", *Technology and Health Care*, vol. 24, pp. S827-S839.

[21] A. Miaskowski and B. Sawicki, (2013) "Magnetic fluid hyperthermia modeling based on phantom measurements and realistic breast model", *IEEE Transactions on Biomedical Engineering*, vol. 60, pp. 1806-1813.

[22] T. Wessapan and P. Rattanadecho, (2016) "Temperature induced in the testicular and related tissues due to electromagnetic fields exposure at 900 MHz and 1800 MHz", *International Journal of Heat and Mass Transfer*, vol. 102, pp. 1130-1140.

[23] L. Wu, J. Cheng, W. Liu, and X. Chen, (2015) "Numerical analysis of electromagnetically induced heating and bioheat transfer for magnetic fluid hyperthermia", *IEEE transactions on magnetics*, vol. 51, pp. 1-4.

[24] E. K. Ng and N. Sudharsan, (2001) "Effect of blood flow, tumour and cold stress in a female breast: a novel time-accurate computer simulation", in *Proceedings of the Institution of Mechanical Engineers, Part H: Journal of Engineering in Medicine*, vol. 215, pp. 393-404.

[25] M. Pavel and A. Stancu, (2009) "Ferromagnetic nanoparticles dose based on tumor size in magnetic fluid hyperthermia cancer therapy", *IEEE transactions on magnetics*, vol. 45, pp. 5251-5254.

[26] C. Ani, Y. Danyuo, O. Odusanya, and W. Soboyejo, (2018) "Computational modeling of drug diffusion and inductive heating in an implantable biomedical device for localized thermo-chemotherapy of cancer cells/tissue", *Cogent Engineering*, vol. 5, p. 1463814.

[27] M. Mital and R. M. Pidaparti, (2008) "Breast tumor simulation and parameters estimation using evolutionary algorithms", *Modelling and simulation in engineering*, vol. 2008, p. 4.

[28] S. Singh and R. Repaka, (2018) "Quantification of thermal injury to the healthy tissue due to imperfect electrode placements during radiofrequency ablation of breast tumor", *Journal of Engineering and Science in Medical Diagnostics and Therapy*, vol. 1, p. 011002.

[29] Y. E. M. A. a. A. G. Saber, (2018) "Temperatures Variation in Different Human Tissues according to Blood Flow Coefficient", *International Journal of Computer Applications*, vol. 180 – No.28.

[30] S. Gabriel, R. Lau, and C. Gabriel, (1996) "The dielectric properties of biological tissues: III. Parametric models for the dielectric spectrum of tissues", *Physics in Medicine & Biology*, vol. 41, p. 2271.

[31] J. L. Meyer, (1984) "The clinical efficacy of localized hyperthermia", *Cancer research*, vol. 44, pp. 4745s-4751s.

[32] E. D. Yıldırım. A mathematical model of the human thermal system. (2005) İzmir Institute of Technology (Turky).

[33] F. Frérart, P. Sonveaux, G. Rath, A. Smoos, A. Meqor, N. Charlier, B. F. Jordan, J. Saliez, A. Noël, and C. Dessy, (2008) "The acidic tumor microenvironment promotes the reconversion of nitrite into nitric oxide: towards a new and safe radiosensitizing strategy", *Clinical Cancer Research*, vol. 14, pp. 2768-2774.

[34] C. M. Sommer, S. A. Sommer, W. O. Sommer, S. Zelzer, M. B. Wolf, N. Bellemann, H. P. Meinzer, B. A. Radeleff, U. Stampfl, and H. U. Kauczor, (2013) "Optimisation of the coagulation zone for thermal ablation procedures: a theoretical approach with considerations for practical use" *International Journal of Hyperthermia*, vol. 29, pp. 620-628.

[35] Y. S. Guan, (2015) "Microwave coagulation therapy of hepatocellular carcinoma", *Hepatoma Res*, vol. 1, pp. 159-64.

[36] E. C. Abenojar, S. Wickramasinghe, J. Bas-Concepcion, and A. C. S. Samia, (2016) "Structural effects on the magnetic hyperthermia properties of iron oxide nanoparticles", *Progress in Natural Science: Materials International*, vol. 26, pp. 440-448.

[37] M. Ansar, S. Atiq, K. Alamgir, and S. Nadeem, (2014) "Frequency and Temperature Dependent Dielectric Response of Fe3O4 Nano-crytallites," *Journal of Scientific Research*, vol. 6, pp. 399-406.

[38] M. Hajiyan, S. Mahmud, M. Biglarbegian, and H. A. Abdullah, (2017) "Natural convection in an enclosure: Effect of magnetic field dependent thermal conductivity", in *Proceedings of the 4th International Conference of Fluid Flow, Heat and Mass Transfer (FFHMT'17)*.

[39] A. M. Gorbach, J. Heiss, C. Kufta, S. Sato, P. Fedio, W. A. Kammerer, J. Solomon, and E. H. Oldfield, (2003) "Intraoperative infrared functional imaging of human brain", *Annals of neurology*, vol. 54, pp. 297-309.